Proton Radiolysis of Carbon Monoxide

By A. R. Anderson, J. V. F. Best and M. J. Willett

Chemistry Division, A.E.R.E. Harwell, Berks.

Received 20*th July*, 1965

The radiation chemistry of CO has been studied, using principally low-energy protons from a Van de Graaff accelerator, as a function of dose rate, temperature and small amounts of additives (CO_2 and O_2). At dose rates higher than those used in previous work a true dose-rate inhibition effect has been found which is interpreted on the basis of competition between second-order and first-order processes. The effect of CO_2 on yields is negligible at concentrations up to 0·5 % by volume but initial yields are extremely sensitive to traces of O_2, particularly at low dose rates.

Increased temperature reduces yields of solid and increases yields of CO_2, but this effect is controlled mainly by subsequent thermal decomposition of the solid. The empirical composition of the solid is unaffected by changes in dose rate, and varies from $(C_3O_2)_n$ at room temperature to essentially pure carbon at temperatures $>450°C$. Nucleation of the solid occurs predominantly in the gas phase. The relative importance of ionic and excitation processes is discussed.

Previous work on the radiolysis of CO is not extensive, but the general features of the reaction are well-established; CO decomposes to produce CO_2 and a carbonaceous solid of variable composition.[1] Similar behaviour is observed with u.-v. light, electrical discharges and microwave radiation.[2]

Little is known about the effects of various parameters, e.g., dose rate, pressure, temperature, extent of decomposition, presence of additives, on the radiolysis of CO, and any ideas on mechanism are necessarily speculative. The initial decomposition yield is not clearly established for while Lind [1] quotes values of $(-M(CO)/N)$ for Rn α-radiation ranging from 1·85 to 6, i.e., $G(-CO) = 6{\cdot}05\text{-}19{\cdot}6$ based on $W_{CO} = 30{\cdot}6$ eV[3], more recent work indicates that the true initial yield is closer to the lower of these limits. Marsh [4] calculates $G(-CO)_{\text{initial}} \sim 6$ from reactor irradiations to high dose, Johnson [5] finds $G(CO_2)_{\text{initial}} = 2{\cdot}3 \pm 0{\cdot}3$ for ^{60}Co γ radiation, corresponding to $G(-CO) \sim 9$ based on the stoichiometry $4nCO \rightarrow nCO_2 + (C_3O_2)_n$, Dondes *et al.*[6] give $G(CO_2) = 1{\cdot}9$ and $G(-CO) = 9{\cdot}3$ for γ-radiation. Moreover, Johnson [5] has demonstrated an efficient ion-induced chain mechanism in the radiolytic oxidation of CO, which implies that initial yields for CO radiolysis can be markedly influenced by traces of O_2.

It has been suggested that inhibition of CO radiolysis with build-up of reaction products is due to two processes, viz., oxidation of the carbonaceous solid,[1, 4] and a charge-transfer process [1] $CO^+ + CO_2 \rightarrow CO_2^+ + CO$ leading to quantitatively different results on the charge neutralization. Both these processes could be important, but Marsh [4] found no evidence for the latter; neither did Lind and Rudolph [7] detect any approach to a quasi-steady state at 50 % conversion. In addition, the latter authors [8] did not find any inhibition of CO radiolysis by Xe, as would be predicted by this mechanism, but the role of energy transfer from rare gases has been further elucidated. It is suggested [6] that the principal energy transfer process is from excited states of the inert gas. Only fragmentary results are available concerning the yield and composition of the solid, and no systematic studies of the effects of dose rate, temperature etc., have been made. The solid formed by irradiation at room temperature appears to have an empirical composition between C_2O and C_3O_2, deduced principally from stoichiometry, and there are no reports of analysis of the solid without previous exposure to moist air. Lind and Bardwell [9] suggested that the solid is a mixture of C and C_3O_2, but it seems improbable that elemental carbon and a carbon-oxygen complex are formed simultaneously.

The present paper describes studies on the radiation chemistry of CO using low-energy protons (~1·5 MeV) from a Van de Graaff accelerator; product yields and changes in the nature of the carbonaceous solid have been studied principally as a function of dose rate, temperature, percentage decomposition, and the presence of trace additives such as O_2 and CO_2.

EXPERIMENTAL

The proton irradiations were carried out with a 2 MeV Van de Graaff accelerator (High Voltage Corporation) equipped with a resolving magnet and collimating system [10] giving an output beam current ranging from 0·003 to 0·7 μA. These currents correspond approximately to dose rates of $6{\cdot}5\times10^{15}$-$1{\cdot}5\times10^{18}$ eV cm^{-3} sec^{-1} ($5{\cdot}2\times10^{18}$-$1{\cdot}2\times10^{21}$ eV g^{-1} sec^{-1}) in CO at s.t.p. for 1·5 MeV protons, but the precise dose rate corresponding to a given current and proton energy depends on energy loss in the cell window. Most of the work was carried out with a gas pressure of 30 cm, but dose rates quoted throughout refer to CO at s.t.p. in order to avoid confusion as the temperature is varied. For γ-ray irradiations a 300 curie ^{60}Co source was used at a dose rate of ~2×10^{12} eV cm^{-3} sec^{-1}.

The diameter of the proton beam on entering the cell was between $\frac{1}{32}$ in. and $\frac{1}{8}$ in., depending upon the apertures in use in the collimator. For most of this work, at 30-40 cm gas pressure and proton energy ~1·5 MeV, the range was ~10 cm and the maximum beam diam. 2 cm. The total heat input at maximum current was only 1 W, and under normal conditions we have calculated that a maximum temperature of ~70°C exists in the discharge zone when the cell walls were at 20°C.

The actual dose rate within the discharge depends upon the distance along the proton track, since the stopping power of the gas varies inversely with the proton energy. But since the discharge becomes wider and more diffuse near the end of the proton range due to scattering, the dose rate per unit volume varies only by a factor of 4 over the major portion of the irradiated volume. The irradiated volume as shown by the beam profiles photographed under various conditions was used to calculate the mean dose rates which are quoted subsequently.

The incident energy of the proton beam was checked by observing the thresholds for the ^{7}Li (p,n) ^{7}Be and ^{3}H (p,n) ^{3}He reactions with a paraffin-wax moderated BF_3 proportional counter and a suitable scaler. For mica windows, the energy lost in the cell window was calculated [11] from the known thickness of material, but for glass and silica windows this loss was determined by actual range measurements and also by irradiating pure gas under well-established conditions to check the yields. The beam current was measured by inserting a platinum or tungsten electrode into the cell just outside the discharge region and connecting this to a d.c. current integrator giving the total charge input in coulombs. Since the cell and window are constructed of insulating materials and the measured correction for forward-scattered electrons was less than 0·2 % with the three windows used (~3 mg cm^{-2}), the above method gives a true total charge input. Before starting an irradiation a removable quartz target, thick enough to absorb the complete beam, was positioned at the exit of the collimator. When a steady beam of the required current was observed on this target, the current integrator was switched to the cell electrode and the quartz target removed for the period of irradiation required. Dosimetry of the ^{60}Co γ-irradiation was based on ferrous sulphate oxidation,[12] $G = 15{\cdot}6$, correcting to the electron density of CO relative to 0·8 N H_2SO_4.

All Van de Graaff cells were made from 1-in. bore standard Pyrex or silica pipe connections in order to make a reproducible and robust fitting to the collimator. Cells were usually 6 in. long with 2 gas connections, one at each end, and an electrode insert. The end remote from the window was made flat wherever possible to permit a clear view of the beam. Mica windows were cemented with Araldite over a $\frac{1}{4}$-in. hole in a circular glass disc and were held by a brass washer on the high vacuum side (fig. 1A). The mica was cleaved from thick sheets and cut into pieces approximately 1 in. square, which were carefully weighed and measured. Samples between 2 and 3 mg cm^{-2} were used for making windows.

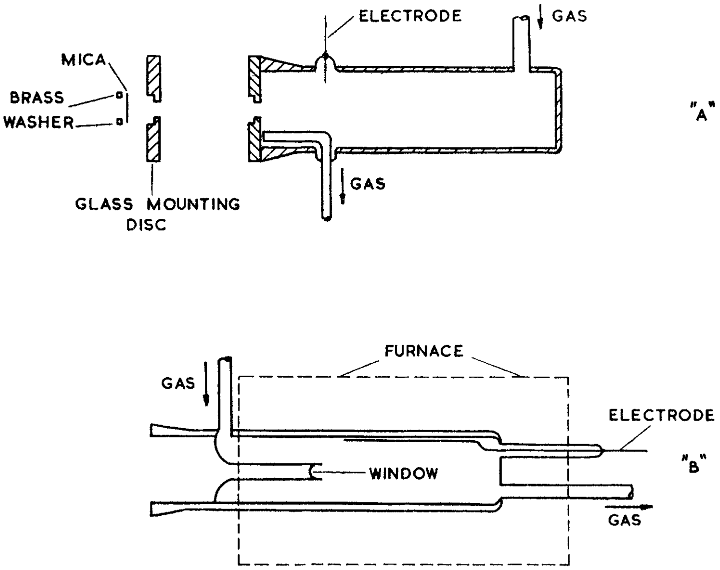

FIG. 1.—Irradiation cells.

A, typical cell for room temperature irradiations; B, Pyrex or silica cell for high temperature irradiations.

The glass and silica windows were primarily intended for high-temperature work, and for this purpose the cells were redesigned. In order to heat the gas in the vicinity of the window and yet preserve the O ring seal to the collimator, the window was sealed by fusion to the end of a re-entrant tube 5 cm long (fig. 1B). Silica windows proved more difficult to make, but could be used over a much wider temperature range. Completely fused all-silica cells were used, with windows made by sandwiching small sections of silica " foil ", previously selected to have a thickness of 0·012 mm, between two sections of 5 mm silica tube and fusing the whole together by induction heating in an inert atmosphere. The window was given a deliberate " bow " and the tube on one side was ground off to a 5 mm stub. These windows withstand a pressure differential of at least 1 atm provided that the higher pressure is applied to the concave side of the window. Pyrex windows have been made by a similar method. The thickness of a glass or silica window cannot be relied upon to remain unchanged during fusion to its mounting tube, and the energy loss in the window was therefore calculated from observed decomposition yields of CO measured under previously well-established conditions. For irradiations at high temperature a well-insulated d.c. furnace was used, since a.c. pick-up from the furnace windings caused inaccuracies in the beam current measurements.

Cells for ^{60}Co γ-irradiations were cylindrical bulbs of 90-100 ml capacity, with a diaphragm type break-seal and a capillary side-tube for attaching to a filling manifold. These were irradiated at the centre of the ^{60}Co source at a temperature of 25-30°C.

Carbon monoxide was obtained by the following methods. (*a*) Dehydration of formic acid using acetic anhydride and sulphuric acid, followed by two distillations of the CO at liquid O_2 temperature. (*b*) Purification of cylinder gas by passage through a copper-catalyst column[13] to remove oxygen, then two " triple U-traps " at liquid-oxygen temperature to remove CO_2, water vapour and any condensable materials such as iron carbonyls. The gas was finally passed through a silica tube heated to 400°C to decompose any carbonyls remaining in the gas phase. This purification train operated slightly above atmospheric pressure, and the gas from it was allowed to flow to a safe vent via an Elliot Moisture Monitor, followed by a Hersch cell[14] to determine oxygen concentration. The Hersch cell electrolyte was $KHCO_3$, so that the cell could be used with both CO and CO_2 Normally the gas was allowed to flow to waste until both water and oxygen concentrations were <1 p.p.m.; it was then either used to fill a storage bulb or used directly in once-through flow experiments. The gas purification and filling lines were free of Hg.

The products of CO radiolysis are CO_2 and a solid polymer $(C_xO_y)_n$ which is formed in the gas phase as a brown dust cloud which remains in suspension for several minutes after its production has ceased. With a continuous flow of gas through the irradiation cell the polymer could be swept out in suspension and collected on a suitable fine filter (silica wool) downstream of the irradiation zone. By this means it appeared possible to collect >90 % of the polymer formed in the cell. The polymer was analyzed for carbon and oxygen without exposure to air, by vacuum pyrolysis at 900°C followed by oxidation of the residual carbon with excess O_2. Carbon dioxide formed during radiolysis was collected in a triple U trap at liquid-N_2 temperature downstream of the polymer filter in the flow experiments, and in a similar trap after transfer by means of a Toepler pump in the static experiments. In all cases gas analysis was carried out by gas chromatography using molecular sieve or silica gel columns.

Small amounts of oxygen (<350 p.p.m. by volume) were introduced from an electrolytic cell inserted into the purification and flow system. CO which had been purified to remove oxygen was passed through a small cell containing dilute H_2SO_4 and two platinum electrodes. The gas was then dried by the existing cold traps in liquid oxygen. Larger amounts of oxygen were added by bleeding cylinder oxygen directly into the system via an oil-filled manometer-type flowmeter. All these experiments were done with the " once-through " flow system.

RESULTS

INITIAL YIELDS

In order to determine initial yields under all conditions the decomposition of CO was restricted to $<0{\cdot}1$ % with ^{60}Co γ-radiation and, in the proton work, the gas flow system was designed to ensure that no significant concentration of products built up in the irradiated volume; the estimated steady-state concentration of CO_2 in the proton beam varies from 10^{-3} to 0·2 %, depending on dose rate. Mean CO_2 concentrations in the proton beam were estimated at different dose rates by considering the initial rate of CO_2 production ($G(CO_2) \sim 2$), diffusion of CO_2 molecules out of the irradiated volume and subsebuent removal in the flowing gas stream. Results of a computer programme show that steady-state conditions are reached in the irradiated zone less than 25 sec after the beginning of the irradiation, resulting in a non-uniform distribution in which the CO_2 concentration varies by a factor of ~ 5. At the highest dose rate employed, $\sim 10^{18}$ eV cm^{-3} sec^{-1}, the maximum steady-state concentration of CO_2 in the beam is $\sim 0{\cdot}4$ %, with a mean value of $\sim 0{\cdot}2$ %; these values are probably over-estimated, as $G(CO_2)$ falls with increasing dose rate (see below). At the lowest rate used, $\sim 6{\cdot}5 \times 10^{15}$ eV cm^{-3} sec^{-1}, the mean steady-state concentration of CO_2 is $\sim 10^{-3}$ %.

With ^{60}Co γ-radiation at a dose rate of 2×10^{12} eV cm^{-3} sec^{-1}, $G(CO_2) = 1{\cdot}96 \pm 0{\cdot}2$ (fig. 2), in agreement with the value of $G(CO_2) = 2{\cdot}05 \pm 0{\cdot}15$ at the lowest proton dose rate, $\sim 6{\cdot}5 \times 10^{15}$ eV cm^{-3} sec^{-1}. The small positive intercept on the ordinate in fig. 2 is probably associated with traces of O_2. $G(C)_{\text{solid}}$ was not determined from the γ-radiolysis but in the gas flow system at the lowest proton dose rate $G(\mathrm{C})_{\mathrm{solid}} = 5{\cdot}4 \pm 0{\cdot}3$. (Yields of solid are quoted in terms of the number of C atoms in the solid, i.e., $G(\mathrm{C})_{\mathrm{solid}}$, to avoid ambiguity arising from changes in solid composition.)

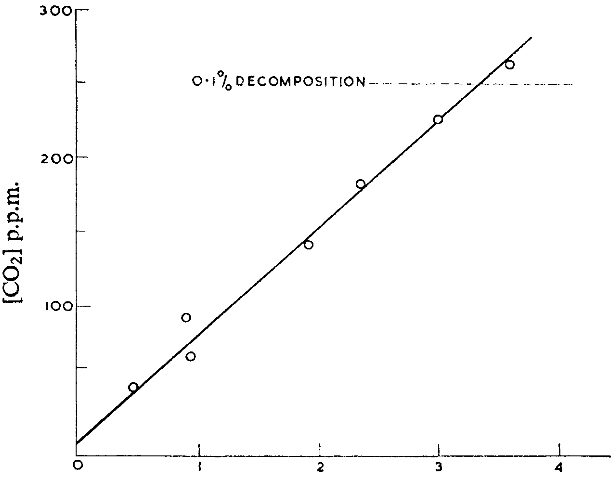

dose (eV cm^{-3} × 10^{-17})

FIG. 2.—Decomposition of CO by ^{60}Co γ-radiation.

dose rate 2×10^{12} eV cm^{-3} sec^{-1}.

EFFECT OF DOSE RATE

Yields of both CO_2 and $(\mathrm{C})_{\mathrm{solid}}$ fall with increasing dose rate over the range $6{\cdot}5 \times 10^{15}$-$1{\cdot}3 \times 10^{18}$ eV cm^{-3} sec^{-1} (fig. 3). In order to confirm that this is a true dose-rate effect and not due to the build-up of products at high dose rates, three supplementary experiments were carried out.

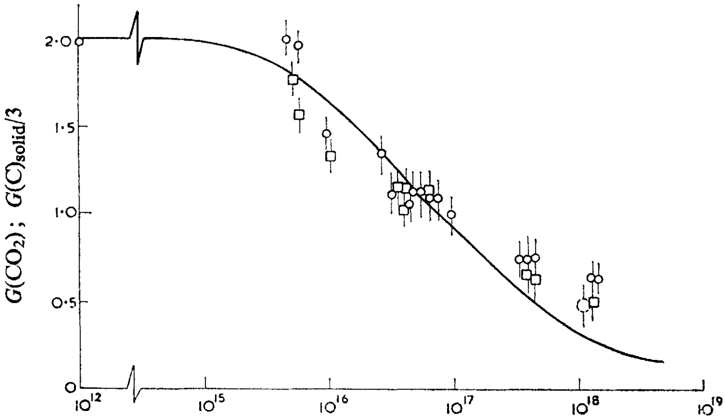

dose rate (eV cm^{-3} sec^{-1})

FIG. 3.—Variation of $G(CO_2)$ and $G(\mathrm{C})_{\mathrm{solid}}$ with dose rate.

line, theoretical ; ○, $G(CO_2)$; □, $G(\mathrm{C})_{\mathrm{solid}}/3$; ◌, estimated correction for temperature effect

CO_2 production in a static system at a dose rate of ~5×10^{17} eV cm^{-3} sec^{-1} increased linearly with dose up to CO_2 concentrations of 0·4 %, compared with an estimated mean steady-state CO_2 concentration in the beam of ~0·08 % in the flow system. This shows that the measured yields in the flow system are initial values. Moreover, wide variation of gas flow rate at the same dose rate produced no significant change in $G(CO_2)$. Addition of 0·5 % CO_2, which is greater than the highest calculated steady-state concentration in any of these experiments, had negligible effect on $G(C)_{solid}$ at a dose rate of 5×10^{16} eV cm^{-3} sec^{-1}, as shown in table 1.

TABLE 1.—EFFECT OF DOSE RATE ON YIELDS

dose rate eV cm^{-3} sec^{-1}	mean $[CO_2]$ at steady state in the beam % by volume	$G(CO_2)$	$G(C)_{solid}$	$G(C)/G(CO_2)$
5×10^{15}	0·0008	2·05±0·15	5·4 ±0·3	2·7
4·23×10^{16}	0·0015	1·48±0·1	4·34±0·2	2·88
2·6×10^{16}	0·003	1·36±0·1		
5×10^{16}	0·008	1·12±0·1	3·33±0·22	2·97
5×10^{16}	0·5 *		3·2	
9×10^{16}	0·014	1·0		
5×10^{17}	0·06	0·78	2·0	2·56
1·3×10^{18}	0·2	0·65	1·5	2·3
1·3×10^{18}		(0·55) †	(1·6) †	(2·91) †

* added initially; † corrected for temperature.

EMPIRICAL COMPOSITION OF SOLID

Changes in dose rate over the above range appear to have little effect on the empirical composition of the carbonaceous solid formed at room temperature. The mean empirical composition of solid formed at 20°C is represented by a ratio of x/y = 1·45±0·07 in the formula $(C_xO_y)_n$; to simplify notation this solid is subsequently referred to as $(C_3O_2)_n$.

MASS BALANCE

In order to check the mass balance in our experiments we have calculated the total amounts of C and O obtained in both the gaseous and solid products. Ideally the C : O ratio should be unity; in practice, we find deviations from unity are generally less than ±10 %, and are often as small as ±2 %. At low dose rates, however, the ratio is extremely sensitive to traces of impurities, and the accuracy in determining it is limited by the smaller amounts of products available for analysis, so that the best mass balance achieved is represented by a deviation from unit C : O ratio of ± 10 %. Results of the mass balance calculations together with the ratios $G(C)_{solid}/G(CO_2)$ in table 1 show that the efficiency of collecting solid in the flow system is >90 %. The decrease in $G(C)_{solid}/G(CO_2)$ ratio at high dose rates is probably associated with an increase in temperature, which leads to enhanced CO_2 production by thermal decomposition of the solid. Heat-transfer calculations indicate that at a dose rate of 1·3×10^{18} eV cm^{-3} sec^{-1} the temperature in the irradiated zone is ~50°C above ambient. Correcting for this increased temperature (see below) reduces $G(CO_2)$ to 0·55 and increases $G(C)_{solid}$ to 1·6, giving a ratio $G(C)_{solid}/G(CO_2)$ = 2·91. On making this correction the empirical composition of the solid is changed from $(C_{1\cdot49}O)_n$ to $(C_{1\cdot36}O)_n$, which is close to the limits for the mean composition over the range of dose rates.

EFFECT OF TEMPERATURE

Increasing the temperature to 300°C at a given dose rate ($\sim 5 \times 10^{17}$ eV cm^{-3} sec^{-1}) produces an increase in $G(CO_2)$ and a corresponding decrease in $G(C)_{solid}$ (fig. 4). Measurements at higher temperatures in the all-silica cells are less reliable at present, due to uncertainties about window thickness, but the data obtained show that $G(CO_2) = G(C)_{solid}$ within experimental uncertainty (± 20 %) at temperatures >450°C. The effect of temperature on yields was examined further in a series of experiments in which gas was irradiated at room temperature and then passed through a heated tube with similar geometry to the irradiation cell but outside the radiation field. Yields obtained in this way depend on gas residence time in the heated zone, but when this residence time is identical with that during irradiations at a given temperature, the yields obtained are similar (fig. 4).

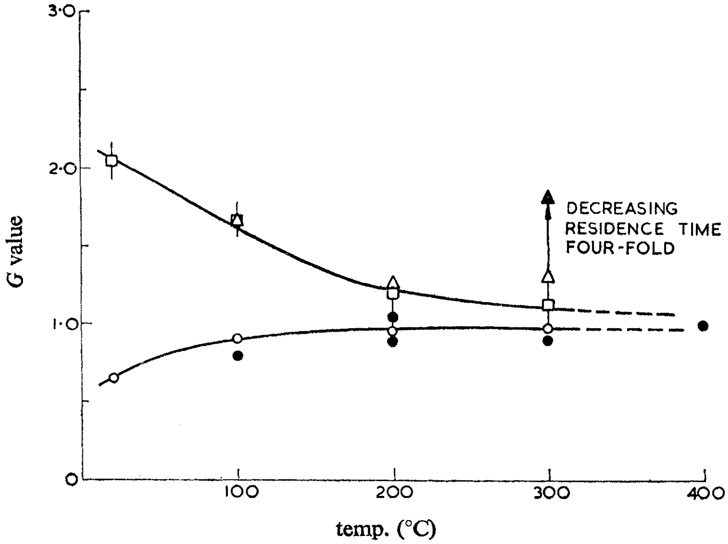

FIG. 4.—Effect of temperature on $G(CO_2)$ and $G(C)_{solid}$.

dose rate $\sim 5 \times 10^{17}$ eV cm^{-3} sec^{-1}

post-irradiation heating: ●, CO_2; △, $(C)_{solid}$ } similar residence time
simultaneous heating and irradiation: ○, CO_2; □, $(C)_{solid}$ }

The carbonaceous solid becomes progressively richer in C with increasing temperature of irradiation and tends towards pure C at temperatures >450°C. (While measured yields above 300°C are subject to ± 20 % uncertainty due to the non-uniform SiO_2 windows, analysis of the solid for empirical composition is not affected by these uncertainties.) Data in fig. 5 show that changes in empirical composition are unaffected by dose rate, and give a good correlation with values calculated from the subsequent pyrolysis of solid formed in irradiations at room temperature. Vacuum pyrolysis of the solid formed in room temperature irradiations produces CO_2 and CO with maxima in the production curves at ~ 300 and ~ 400°C respectively. These measurements were made by heating the solid to a given temperature, removing the gases by a Toepler pump in successive cycles until gas evolution had ceased, and then repeating the process at a higher temperature.

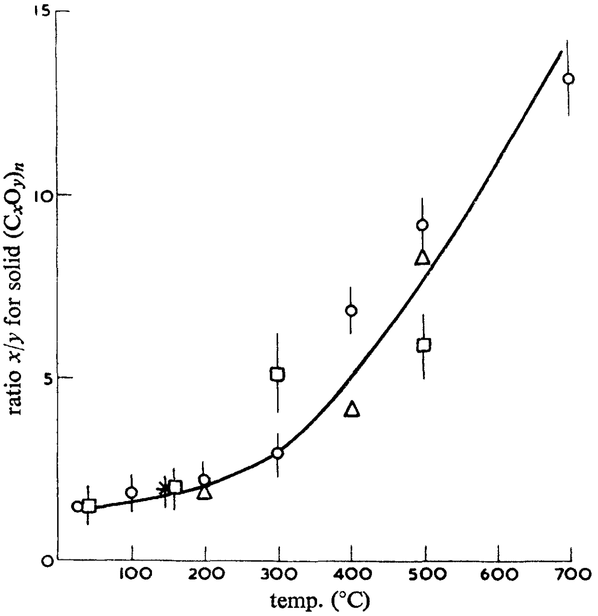

FIG. 5.—Variation with temperature of empirical composition of solid from CO radiolysis. dose rate (eV cm^{-3} sec^{-1}). □, 6×10^{15}; ○, 5×10^{17}; ✱, 10^{15} (ref. (4)); △, composition calculated from pyrolysis of solid formed during irradiation at 20°C.

NUCLEATION PROCESSES

Under the experimental conditions in the present work, nucleation of the solid particles occurs predominantly in the gas phase. Evidence for this conclusion is provided by the following observations. (*a*) Photographs taken during irradiation show clearly that the particulate matter is nucleated in the gas phase. The photograph in fig. 6 is an end view of the irradiation cell with the direction of gas flow perpendicular to the plane of the paper. The " dust cloud " exhibits twin symmetry, due to the combined effect of gas flow and convection currents produced by the heating effect of the proton beam; it is seen that the particulate matter is almost completely isolated from the cell walls. (*b*) The good mass balance in the radiolysis products from the flow experiments shows that >90 % of the solid is carried in the gas stream to the filter trap. (*c*) The similarity of deposits found on a wide variety of electron microscope grids shows that changes in the nature of surfaces have little effect on nucleation processes.[15] (*d*) Measurements of light transmission through the irradiated gas showed that the transmission falls rapidly to a steady-state value during irradiation and rises quickly to >95 % on stopping the irradiation.

EFFECTS OF OXYGEN

Yields of CO_2 and of solid are very sensitive to small concentrations of O_2 (10 p.p.m. by vol.) at low dose rates (fig. 7), but the effect of a given concentration of

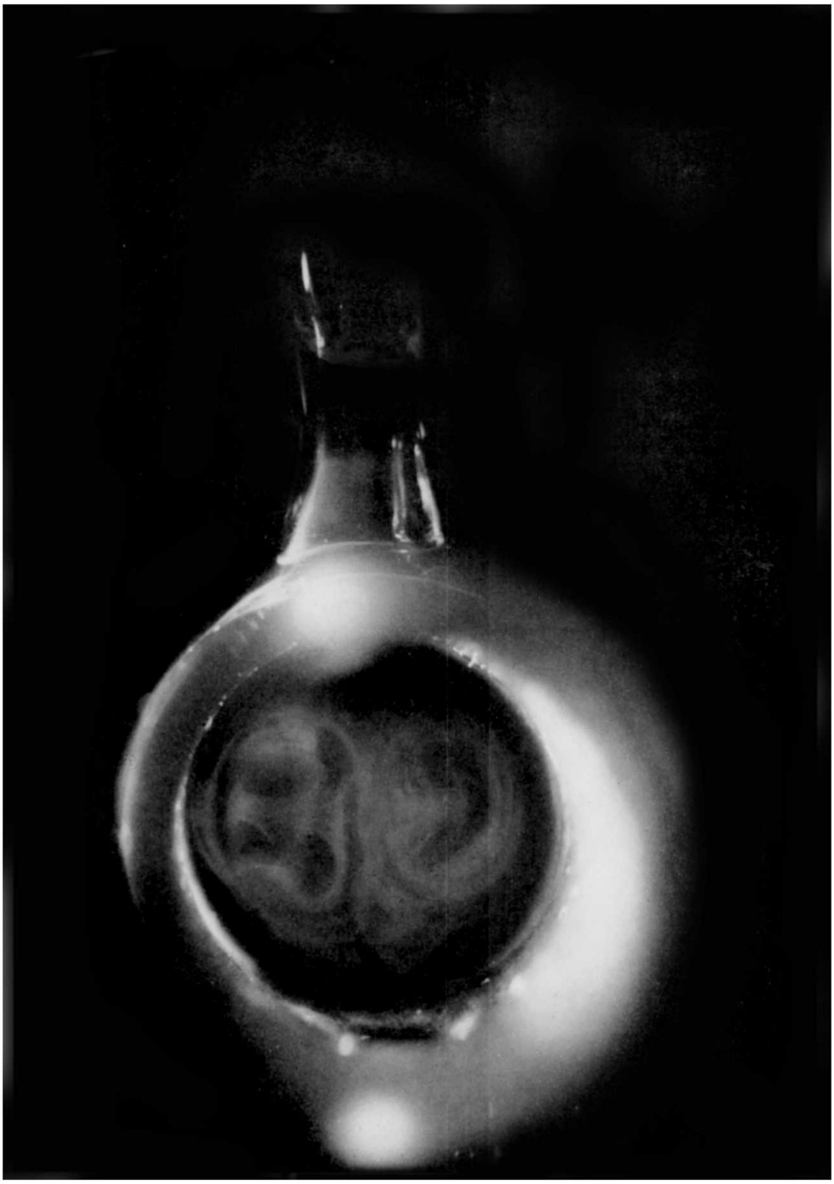

FIG. 6.—Gas-phase nucleation of carbonaceous solid from radiolysis of CO.

O_2 decreases with increasing dose rate. The extreme sensitivity of the measurements to traces of O_2 at low dose rates largely accounts for the poorer mass balance under these conditions. Variation of O_2 concentration up to 2 p.p.m. can have a significant effect on both $G(CO_2)$ and $G(C)_{solid}$.

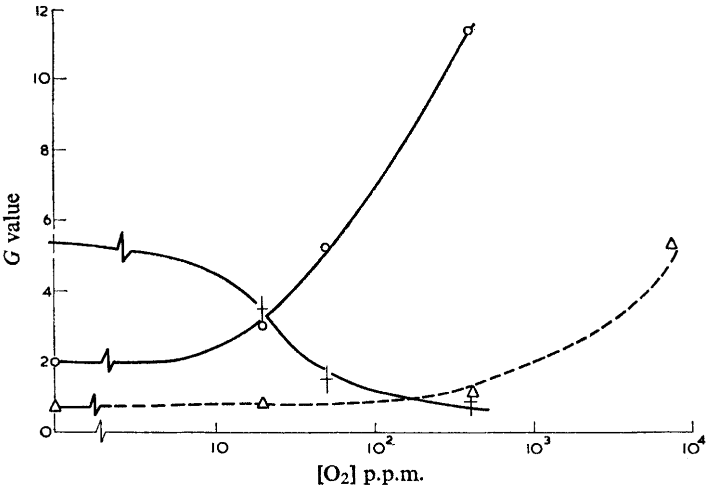

FIG. 7.—Effect of O_2 on yields at different dose rates.

dose rate 6×10^{15} eV cm^{-3} sec^{-1} : ○, $G(CO_2)$; +, $G(C)_{solid}$; dose rate 5×10^{17} eV cm^{-3} sec^{-1} : △, $G(CO_2)$; - - - - - calc. line

DISCUSSION

INITIAL YIELDS

Our value of $G(CO_2) = 1{\cdot}96\pm0{\cdot}2$ with ^{60}Co γ-radiation agrees well with our value for proton radiolysis of $G(CO_2) = 2{\cdot}05\pm0{\cdot}15$ at the lowest dose rate used, also Johnson's value [5] of $G(CO_2) = 2{\cdot}3\pm0{\cdot}3$ and with Dondes' [6] value of $G(CO_2) = 1{\cdot}9$. The ratio $G(C)_{solid}/G(CO_2)\sim3$ for room temperature irradiations over a range of dose rates, together with the empirical analysis of the carbonaceous solid as $(C_3O_2)_n$, determined both in this work and in preliminary studies by Johnson,[16] suggests that the overall stoichiometry is best represented by the expression

$$4nCO \rightsquigarrow nCO_2+(C_3O_2)_n.$$

Thus a mean value of $G(-CO) = 8\pm1$ for the initial disappearance of CO is derived from the present work in conjunction with Johnson's results. This value is close to the initial values found by Lind and Rudolph [7] in the absence of CO_2, viz., $g(-CO) = 8{\cdot}4$-$9{\cdot}6$, and with the value of $G(-CO)\sim6$ calculated for reactor irradiations to high total doses.[4] It does, however, differ markedly from Lind's suggestion [1] that the true initial value is $G(-CO) = 12$-20, and we conclude that these latter measurements were probably affected by traces of oxygen.

The close agreement between results from irradiation with radon α-particles, 1·5 MeV protons, ^{60}Co γ-radiation, and reactor radiation suggests that there is no significant L.E.T. effect at low gas pressures ($\sim$1 atm) over this range of ionization densities.

EFFECT OF DOSE RATE

Our results show that the decrease in yields with increasing dose rate represents a true dose rate effect, and that the yield does not depend on the low percentage decomposition obtaining in the beam at different dose rates. In previous work decreases in $G(-\mathrm{CO})$ have been attributed to build-up of reaction products followed by oxidation of the radiolytic solid by CO_2,[4,9] or to the occurrence of the charge-transfer reaction.[7]

$$CO^+ + CO_2 \rightarrow CO_2^+ + CO$$

Neither of these inhibition processes is adequate to explain our observations in the present work. The data in table 1 show that we are observing inhibition of CO radiolysis at CO_2 concentrations much less than that suggested by Lind and Rudolph to account for inhibition by charge transfer. Moreover, the observed effects cannot be attributed to the concentration of CO_2 alone as shown by results obtained when 0·5 % CO_2 is added at a dose rate of $\sim 5 \times 10^{16}$ eV cm^{-3} sec^{-1}. In addition, subsequent oxidation of the carbonaceous solid by O atoms would depend on the concentration of carbonaceous solid in the irradiated zone, which would be affected by a change in gas flow rates at a given rate of energy input.

Consideration of various possible reaction mechanisms to account for the radiolysis of CO suggests that the decrease in yields at high dose rates is due to reactions involving chemically reactive intermediates such as C_2O, which are not significant at the lower does rates used in previous work.[1, 4]

We consider the following reactions:

$$CO \rightsquigarrow CO^+ + e^- \tag{1}$$

$$CO \rightsquigarrow CO^* \rightarrow C + O \tag{2}$$

$$CO^+ + e^- \rightarrow CO^* \rightarrow C + O \tag{3}$$

$$CO^+ + CO \rightarrow (CO)_2^+ \xrightarrow{CO} (CO)_n^+ \tag{4}$$

$$(CO)_n^+ + e^- \rightarrow nCO \tag{5}$$

$$O + CO \rightarrow CO_2 \tag{6}$$

$$C + CO \rightarrow C_2O \tag{7}$$

$$C_2O + CO \rightarrow C_3O_2 \tag{8}$$

$$C_2O + O \rightarrow 2CO \tag{9}$$

$$C_3O_2 + O \rightarrow CO_2 + C_2O \tag{10}$$

$$C + C + M \rightarrow C_2 + M \tag{11}$$

$$O + O + M \rightarrow O_2 + M \tag{12}$$

$$O + C + M \rightarrow CO + M \tag{13}$$

$$C + CO_2 \rightarrow 2CO \tag{14}$$

Without attempting to distinguish the importance of primary ionization and excitation processes we consider the subsequent reactions of C and O atoms formed in these processes, and demonstrate the dependence of observed yields as a function of dose rate. Re-formation of CO can occur through reactions (9), (13) and (14) with consequent decreases in $G(CO_2)$ and $G(\mathrm{C})_{\mathrm{solid}}$, but our results with varying flow rate and with added CO_2 eliminate reaction (14) from consideration. Thus, the two reactions (9) and (13) leading to the reformation of CO are in competition with the processes (6), (7) and (8) which result in destruction of CO. If k_{12} is typical of the three-body reactions (11), (12) and (13), there is certain *a priori* evidence to suggest that reactions (6) and (7) (first order with respect to [O] and [C]) are rapid compared to the radical-radical reactions (11)-(13) under our conditions of pressure and dose rate. At 20°C, $k_{12} = 10^{-32}$ cm^6 molecule^{-2} sec^{-1},[17] and $k_6 = 2{\cdot}1 \times 10^{-17}$ cm^3 molecule^{-1} sec^{-1},[18] so that at the highest dose rate used, $\sim 10^{18}$ eV cm^{-3} sec^{-1}, the steady-state concentration of O atoms is $\sim 10^{14}$ cm^{-3}, derived from $d(\mathrm{O})/dt = R_0 - k_{12}[\mathrm{O}]^2\mathrm{M} - k_6[\mathrm{O}][\mathrm{CO}]$, where R_0 is the initial rate of production of O atoms. At 20°C and $p(\mathrm{CO}) = 30$ cm Hg the rate of reaction (12) is ~ 4 % of the rate of reaction (6), and the relative rate will decrease with decreasing dose rate.

We make two further assumptions: (*a*) that reaction (7) is rapid, so that the rate of production of C_2O is approximately equal to the rate of production of C atoms; and (*b*) we neglect reaction (10) as [19] $k_9 > k_{10}$. Thus the simplified reaction scheme used to explore the kinetics comprises reactions (1), (2), (3), (6), (7), (8) and (9).

By applying steady-state kinetics it follows that:

$$\mathrm{d}[\mathrm{O}]/\mathrm{d}t = R_0 - k_6[\mathrm{O}][\mathrm{CO}] - k_9[\mathrm{C_2O}][\mathrm{O}],$$

$$\mathrm{d}[\mathrm{C_2O}]/\mathrm{d}t = R_0 - k_8[\mathrm{C_2O}][\mathrm{CO}] - k_9[\mathrm{C_2O}][\mathrm{O}],$$

where R_0 is the initial rate of production of O and C_2O.

At the steady state,

$$[\mathrm{O}] = \frac{k_6k_8[\mathrm{CO}]}{2k_9k_6}\left\{\left(1+\frac{4k_9k_6R_0}{k_8(k_6[\mathrm{CO}])^2}\right)^{\frac{1}{2}}-1\right\},$$

$$\therefore \quad \frac{\mathrm{d}[\mathrm{CO_2}]}{\mathrm{d}t} = \frac{(k_6[\mathrm{CO}])^2k_8}{2k_9k_6}\left\{\left(1+\frac{4k_9k_6R_0}{k_8(k_6[\mathrm{CO}])^2}\right)^{\frac{1}{2}}-1\right\}. \qquad \text{(A)}$$

By substituting $K = k_9k_6/k_8$ and $F = KR_0/(k_6[\mathrm{CO}])^2$,

$$\mathrm{d}[\mathrm{CO_2}]/\mathrm{d}t = (R_0/2F)[(1+4F)^{\frac{1}{2}}-1]. \qquad \text{(B)}$$

This expression is in the same form as that developed to interpret general dose-rate effects in radiation chemistry [20] and can be written in the form

$$S = [(1+4F)^{\frac{1}{2}}-1]/2F,$$

where S is the fraction of O atoms which take part in the first-order reaction (6). At low dose rates, S will be essentially unity, and at high dose rates it will tend to zero as $G(\mathrm{CO_2})$ tends to zero. When $S = 0{\cdot}5$, $F = 2$, and this value of F defines the dose rate at which the rates of reactions (6) and (9) are equal. Inspection of fig. 3 shows that the dose rate at which $S = 0{\cdot}5$ is $\sim 6 \times 10^{16}$ eV cm^{-3} sec^{1}, from which we derive a value of $K = k_9k_6/k_8 = 7{\cdot}3 \times 10^{-11}$ cm^3 molecule^{-1} sec^{-1}. $R_0 = G(\mathrm{O}) \times 10^{-2} \times D$ atoms cm^{-3} sec^{-1}, where $G(\mathrm{O})$ is the initial yield of O atoms in the dose-rate independent region, taken as equal to $G(\mathrm{CO_2})_{\mathrm{initial}}$, and D is the dose rate in eV cm^{-3} sec^{-1}. We can now calculate F at all dose rates and so derive a theoretical curve for variation of $G(\mathrm{CO_2})$ with dose rate from eqn. (A) and (B). The calculated curve in fig. 3 is in reasonable agreement with the experimental data; values of $G(\mathrm{C})_{\mathrm{solid}}/3$ are also included. With the more extensive data for $G(\mathrm{CO_2})$, however, it is seen that the experimental points lie above the theoretical line at high dose rates, although the general sigmoid form of the relationship is retained. This divergence at high dose rates could be a manifestation of the approximations used in deriving the kinetics or it could be associated with a temperature effect, as the temperature of the gas in the irradiated volume is estimated as ~ 70°C at a dose rate of $\sim 1{\cdot}3 \times 10^{18}$

eV cm^{-3} sec^{-1}. Our data on the effect of dose rate with increasing temperature are limited, but we can use them to estimate a possible correction as shown in fig. 3. At the lower dose rates used, the gas temperature is not significantly above ambient.

The good correlation between the experimental data and the proposed reaction scheme does not exclude the participation of other reactions of ions or neutral fragments since several alternative mechanisms could satisfy the final kinetic expression. Excited CO* molecules could react via reactions (15) and (16),

$$CO^* + CO \rightarrow CO_2 + C \tag{15}$$

$$CO^* + CO \rightarrow C_2O + O, \tag{16}$$

which would be formally equivalent to reactions (2) and (3) followed by reactions (6) and (7). With molecules in the electronic ground-state, reaction (15) is endothermic to the extent of ~6 eV, but would take place with the lowest excited triplet level of CO ($a^3\pi$ at 6·03 eV). While the heat of formation of C_2O is not known, Harteck *et al.*[21] argue that a higher excited state of CO is required for reaction (16) to occur, but it could participate in the radiation-chemical reaction. The fate of the primary ions has not been clearly established, but it would appear from the rates for ion-electron recombination[22] that simple charge recombination (eqn. (3)) is unlikely to predominate at pressures near atmospheric. The ion-molecule reactions (17)-(21) have been demonstrated in the mass spectrometer,[23, 24]

$$CO^+ + CO \rightarrow C_2O_2^+ \tag{17}$$

$$CO^+ + CO \rightarrow C_2O^+ + O \tag{18}$$

$$CO^+ + CO \rightarrow CO_2^+ + C \tag{19}$$

$$CO^+ + CO \rightarrow C^+ + O + CO \tag{20}$$

$$CO^+ + CO \rightarrow C + O^+ + CO. \tag{21}$$

In addition the existence of $C_2O_2^+$ is required for the interpretation of ion drift velocity experiments,[25] and it can also be formed[23] in reaction (22),

$$CO^* + CO \rightarrow C_2O_2^+ + e^-. \tag{22}$$

The relative importance of ions and excited states in the radiolysis of CO was discussed by Stewart and Bowlden,[26] who claimed that their interpretation of results in the presence of rare gases demonstrated that ionization plays an important role in the process. However, Dondes *et al.*[6] have suggested that in the presence of rare gases the most important process is connected with the probability of energy transfer from the excited rare-gas atom to specific singlet and triplet levels in the CO molecule. This suggestion, that the radiolysis of CO is controlled principally by the dissociation of excited CO molecules or by their reaction with ground-state CO molecules, may explain the inefficient utilization of energy in the radiolysis. If each primary CO^+ ion could produce a CO_2 molecule through eqn. (1), (3) and (6) then $G(CO_2) = 3·27$ from ionic processes, taking $W(CO) = 30·6$ eV.[3] Since the ionization potential of CO is 14·0 eV, additional dissociative processes will arise from the excess energy of 16·6 eV per ionization event. Some of this additional energy will produce excited ionic states, but an estimate of the CO_2 yield from excited CO molecules could be made by considering photochemical data. Groth[27] *et al.* found a quantum yield of about unity for CO disappearance ($\phi(CO_2) \sim 0·25$) at 1295 Å (~9·6 eV), where virtually all the states of CO up to the dissociative level (11·1 eV) can be excited. Harteck *et al.*[21] found ϕ (CO_2) " between a few tenths and unity " using the 2062 Å line of iodine (~6·9 eV) and attributed this to specific excitation of CO to the $a^3\pi$ level. Excited levels of CO from 6·03 eV to 11·11 eV are known from spectroscopic data,[28] and for the purpose of this estimate we assume a mean excitation level of 8·5 eV and use Groth's value for ϕ (CO_2), as this is derived over a wider range of excited states of CO than is Harteck's value. This leads to a yield of CO_2 from excitation processes, $G(CO_2) = 1{\cdot}60 \pm 0{\cdot}4$, where the limits of error reflect the uncertainty in the assumed value for mean excitation energy. As chemical reaction with the lower excited state is more probable, the upper limit is perhaps the better approximation. Thus, the total calculated yield of CO_2 in the radiolysis of CO is $G(CO_2) \sim 4{\cdot}9$, which is more than double the observed initial yield at low dose rates. If we can largely neglect the contribution from ionic processes to CO radiolysis the value of $G(CO)_2$ calculated from excitation processes is close to the observed value.

In view of the ion-molecule reactions which have been shown to occur in ionized CO it is unlikely that the simple dissociative recombination (eqn. (3)) predominates. In addition, complexes [29] between ions and neutral molecules are important even at pressures <10 mm Hg. If, therefore, the dominant recombination reaction involves species such as $C_2O_2^+$ or $(CO)_n^+$, neutralization is not necessarily dissociative, as the energy released can be shared between several molecules in the cluster, e.g., equal distribution of the recombination energy between three CO molecules will not produce electronic excitation to the lowest level (6·03 eV). This suggests that ions do not play an important role in determining the ultimate chemistry in the radiolysis of CO; the postulate may have wider application to other gaseous systems.

FORMATION OF SOLID

The processes leading to the formation of solid in the radiolysis of CO are not well established, but it appears from infra-red absorption studies that the condensation and nucleation processes are not due simply to bimolecular collisions between C_3O_2 molecules. The infra-red spectrum [30, 31] of thermally and photochemically polymerized C_3O_2 shows two distinct bands at $\sim 6{\cdot}9\ \mu$ and $12{\cdot}4\ \mu$ which are probably characteristic of a lactone ring structure, but which are absent in the solid produced by CO radiolysis. The only characteristic absorption band shown by the latter is a typical $—C=O$ vibrational band at $5{\cdot}6\ \mu$ which shifts to $5{\cdot}8\ \mu$ on hydration.[32] This suggests that the carbonaceous solid formed from CO radiolysis does not have the same closed-ring structure proposed by Smith *et al.*[30] for C_3O_2 polymer, but may consist of linear polymer units cross-linked by C—C bonds although there is insufficient evidence to write a detailed structure.

Our extensive evidence in support of gas-phase nucleation demonstrates the validity of Lind's assumption [1] that the primary reactions resulting in solid formation occur in the gas phase. Subsequent deposition and aggregation of the solid on surfaces will, however, be a complex function of surface condition, surface material, temperature and hydrodynamics. In addition, nucleation processes at walls may compete with gas phase nucleation at low dose rates, depending on the wall material and temperature.

EFFECT OF TEMPERATURE

Increases in $G(CO_2)$ and decreases in $G(C)_{solid}$ with increasing temperature at a given dose rate appear to be controlled principally by thermal decomposition of the solid to yield CO_2 and a progressively carbon-rich solid. Our observations on the composition of the solid are consistent with the view that the solid formed during radiolysis of CO is primarily $(C_3O_2)_n$, at all dose rates, and that changes in composition with temperature are principally due to subsequent thermal decomposition (fig. 5). This is demonstrated by the pyrolysis of solid formed by irradiation heating flow experiments. As the composition of the solid tends towards pure carbon, $G(CO_2)$ should tend towards $G(C)_{\text{solid}}$ according to the overall stoichiometry,

$$2CO \rightarrow CO_2 + C,$$

and this has been demonstrated within experimental error. The general trend of empirical composition with temperature at different dose rates and the excellent agreement of data from irradiations in the Harwell reactor DIDO[4] (fig. 5) are consistent with the postulate that dose-rate dependent inhibition processes occur at an early stage in the radiolysis.

EFFECT OF OXYGEN

Johnson *et al.*[5] have postulated the existence of an ionic chain mechanism to explain the radiation-induced oxidation of CO, which is independent of dose rate over the range which they studied, viz., 2×10^{11} eV cm^{-3} sec^{-1}-5×10^{12} eV cm^{-3} sec^{-1}. At the high dose rates used in the present work, however, charge recombination between electrons and any positive ion[29] could begin to compete with chain initiation by charge-transfer reactions at low concentrations of O_2.

The characteristic times for charge-transfer reactions and volume charge recombination processes are given[22] respectively by Kp^{-1} and $K'(p'I)^{-\frac{1}{2}}$, where p is the partial pressure of O_2 and p' is the total gas pressure in atmospheres; I is the rate of energy absorption in eV g^{-1} sec^{-1}. It follows that competition between the two processes at constant total gas pressure is governed by

$$dR_{CT}/dR_{CR} \propto dp/d(I)^{\frac{1}{2}}$$

where R_{CT} and R_{CR} are the respective rates of the charge transfer and charge recombination reactions. This equation predicts that with an increase of dose rate by dx, the partial pressure of oxygen must be increased by $(dx)^{\frac{1}{2}}$ to give the same proportional effect on $G(CO_2)$. In fig. 7 the theoretical line for the effect of O_2 at a dose rate of $\sim 5\times10^{17}$ eV cm^{-3} sec^{-1} has been calculated on this basis from the data obtained at a dose rate of $\sim 5\times10^{15}$ eV cm^{-3} sec^{-1}, and gives good agreement with the experimental data. The postulated competition will be unimportant at low dose rates, as our data indicate that in Johnson's work[5] at a dose rate of 2×10^{11} eV cm^{-3} sec^{-1} the chain initiation charge-transfer reactions will compete efficiently with charge recombination reactions at O_2 concentrations >1 p.p.m.

We acknowledge helpful discussions with Dr. C. B. Amphlett and Dr. W. G. Burns during the course of this work. Thanks are also due to Mr. B. Morris for operation of the Van de Graaff accelerator, and to Mr. A. M. Deane who carried out the i.-r. measurements.

[1] Lind, *Radiation Chemistry of Gases*, A.C.S. Monograph, no. 151 (Reinholt Publishing Corp., New York, 1961).
[2] Glockler and Lind, *Electrochemistry of Gases and Other Dielectrics* (Chapman and Hall Ltd., London, 1939).
[3] Riegler and Rudloff, *Ann. Physik*, 1955, **15**, 224.
[4] Marsh and Wright, 1964, *Harwell Research Report* no. AERE-R4198.
[5] Johnson, Clay and Warman, *Disc. Faraday Soc.*, 1963, **36**, 46.
[6] Dondes, Harteck and Weyssenhoff, *Z. Naturforsch*, 1964, **19a**, 13.
[7] Lind and Rudolph, *J. Chem. Physics*, 1960, **33**, 705.

[8] Lind and Rudolph, *J. Chem. Physics*, 1961, **34,** 1572.

[9] Lind and Bardwell, *J. Amer. Chem. Soc.*, 1925, **47,** 2675.

[10] Burns, *Trans. Faraday Soc.*, 1962, **58,** 961.

[11] Allison and Warshaw, *Rev. Mod. Physics*, 1953, **25,** 779.

[12] Hochanadel and Ghormley, *J. Chem. Physics*, 1953, **21,** 880.

[13] Meyer and Ronge, *Angew. Chem.*, 1951, **52,** 637.

[14] Hersch, *Inst. Practice*, 1957, **11,** 817, 937.

[15] Dawson, I. M., unpublished work.

[16] Johnson, private communication.

[17] Morgan, Elias and Schiff, *J. Chem. Physics*, 1960, **33,** 930.

[18] Mahan and Solo, *J. Chem. Physics*, 1962, **37,** 2699.

[19] Sutton, Faraggi and Schmidt, *J. Chim. Physique*, 1960, **57,** 643.

[20] Burns and Barker, 1963, *Harwell Research Report* no. AERE-R4240.

[21] Harteck, Reeves and Thompson, *Z. Naturforsch.*, 1964, **19a,** 2.

[22] Hart and Platzman, *Mechanisms in Radiobiology* (Academic Press, New York, 1961), vol. 1, chap. 2.

[23] Munsen, Field and Franklin, *J. Chem. Physics*, 1962, **37,** 1790.

[24] Melton and Wells, *J. Chem. Physics*, 1957, **27,** 1132.

[25] Varney, *Physic. Rev.*, 1953, **89,** 708.

[26] Stewart and Bowlden, *J. Physic. Chem.*, 1960, **64,** 212.

[27] Groth, Faltings and Harteck, *Z. physik. Chem. B*, 1938, **41,** 15.

[28] Herzberg, *Spectra of Diatomic Molecules* (D. van Nostrand Company, New York, 1950).

[29] Mahan and Person, *J. Chem. Physics*, 1964, **40,** 392. Calton and Mahan, *J. Chem. Physics*, 1964, **40,** 3683.

[30] Smith, Young, Smith and Carter, *Inorg. Chem.*, 1963, **2,** 829.

[31] Blake, Eeles and Jennings, *Trans. Faraday Soc.*, 1964, **60,** 691.

[32] Deane, unpublished work.